# Direct observation of current-induced conductive path in colossal-electroresistance manganite thin films

Wengang Wei,[1,2] Yinyan Zhu,[1] Yu Bai,[1] Hao Liu,[1] Kai Du,[1] Kai Zhang,[1] Yunfang Kou,[1] Jian Shao,[1] Wenbin Wang,[1] Denglu Hou,[2] Shuai Dong,[3] Lifeng Yin,[1,4,*] and Jian Shen[1,4,†]

[1]*State Key Laboratory of Surface Physics and Department of Physics, Fudan University, Shanghai 200433, China*
[2]*College of Physics and Information Engineering, Hebei Normal University, Shijiazhuang 050024, China*
[3]*Department of Physics, Southeast University, Nanjing 211189, China*
[4]*Collaborative Innovation Center of Advanced Microstructures, Nanjing 210093, China*
(Received 7 October 2015; revised manuscript received 30 November 2015; published 12 January 2016)

Manganites are known to often show colossal electroresistance (CER) in addition to colossal magnetoresistance. The $(La_{1-y}Pr_y)_{1-x}Ca_xMnO_3$ (LPCMO) system has a peculiar CER behavior in that little change of magnetization occurs. We use a magnetic force microscope to uncover the CER mechanism in the LPCMO system. In contrast to the previous belief that current reshapes the ferromagnetic metallic (FMM) domains, we show that the shape of the FMM domains remain virtually unchanged after passing electric current. Instead, it is the appearance of a tiny fraction of FMM "bridges" that is responsible for the CER behavior.

For perovskite manganites, it has been known that their physical properties depend sensitively on external stimuli including magnetic field [1,2], electric field [3–5], strain [6,7], pressure [8], light [9,10], and current [11–15]. The current-induced effect is of particular interest for potential electronic device applications. Previously, it has been reported that current can lead to a large drop of resistivity [12] and a significant increase of magnetization [14] in the $Pr_{1-x}Ca_xMnO_3$ system, which has been understood as current-induced transition from a charge-ordered insulating (COI) state to a ferromagnetic metallic (FMM) state. The effect of current, however, appears to be quite different in the $La_{5/8-y}Pr_yCa_{3/8}MnO_3$ (LPCMO) system. While current still can induce a large drop of the resistivity, little change of the magnetization was observed [15]. This is somewhat puzzling considering the fact that spin and charge are strongly coupled in manganites systems.

Based on a dielectrophoresis model calculation [16], Dong *et al.* proposed that the current reshape the FMM domains without changing their actual volume fraction, which can assist percolation of the FMM metallic domains to form conducting pathways. Later experimental work showed that current led to anisotropic transport behavior in the LPCMO systems [17], which indirectly supports the dielectrophoresis model.

In this work, while confirming previous experimental observations [15,18] that current can induce a large drop of resistivity but little change of magnetization in the LPCMO system, we show direct evidence to uncover the mechanism for the colossal electroresistance in LPCMO. Using a magnetic force microscope (MFM), we show that current does not change the shape of the FMM domains, but rather causes a few small FMM domains to appear at critical regions to bridge large neighboring FMM domains. Although the tiny addition of FMM domains does not lead to a noticeable increase in the global magnetization measurement, they can generate several

orders of magnitude drop of resistivity based on our resistive network simulation.

Sixty-nm $(La_{2/3}Pr_{1/3})_{5/8}Ca_{3/8}MnO_3$ films were epitaxially grown on (001)-oriented $SrTiO_3$ (STO) substrates using laser molecular beam epitaxy (248 nm, 2 Hz, $2\,J/cm^2$ fluence) in flowing oxygen atmosphere (8% ozone) of about $3.0 \times 10^{-3}$ mbar. The substrate temperature was kept at $800\,°C$ to allow an atomically flat growth front, which produced a thin film with high quality. After growth, samples were annealed in a furnace with flowing oxygen at a pressure of 1 atmosphere at $950\,°C$ for 3 hours to optimize the oxygen content. The quality of the thin films was examined by *in situ* reflection high-energy electron diffraction, *ex situ* atomic force microscope, and x-ray diffraction (see supplementary material [19]). MFM images and the transport measurements were carried out in Physical Property Measurement System with Scanning Probe Microscope (PPMS-SPM). Details of MFM measurements are described elsewhere [20]. A superconducting quantum interference device was used for magnetic property measurements.

The dramatic current effect on the transport properties of the LPCMO films is already obvious when changing the measuring current. Figure 1(a) shows the temperature-dependent resistivity of a LPCMO film at different measuring current density. Increasing the measuring current density by four orders of magnitude leads to an 80-K increase of the metal-insulator transition temperature ($T_{MIT}$) and three orders of magnitude drop of resistivity below $T_{MIT}$. Here we note that the large current effect is not related to Joule heating, which should lead to the opposite change of $T_{MIT}$. In fact, the Joule heating effect is negligible in our measurements, as confirmed by the fact that the *R-T* curves measured by pulsed current (10-ms pulse width, 5 s interval) and continuous current with the same current density ($2 \times 10^4\,A/cm^2$) are nearly identical [see Fig. 1(a)].

To further examine the current effect on transport, we measured the dependence of resistivity on the sweeping sequence of current at fixed temperatures of 10, 80, and 150 K, as shown in Figs. 1(b)–1(d), respectively. In all three cases, the sample was cooled from room temperature to the measuring temperature under zero current prior to

---

*To whom correspondence should be addressed: lifengyin@fudan.edu.cn
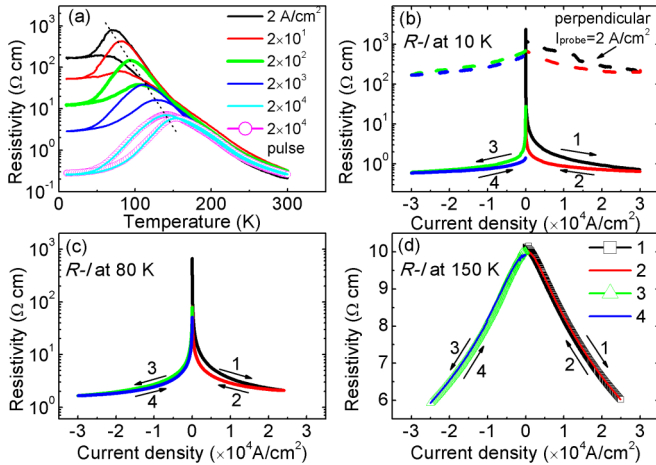
†shenj5494@fudan.edu.cn.

FIG. 1. (a) Temperature-dependent resistivity measured by different current density. The almost identical curves of pulsed and continuous current indicate that Joule heating effect at $2 \times 10^4$ A/cm$^2$ is negligible. The dashed line marks the increasing of MIT temperature with the current density. Panels (b), (c), and (d) are the $R$-$I$ curves acquired after zero-current cooling to 10, 80, and 150 K, respectively. The arrows indicate the sweeping sequence of the current. The dashed line in panel (b) is the resistivity in the perpendicular direction detected by a small current density during the sweeping sequence.



FIG. 2. Initial magnetization curves and *M-H* loops with zero current cooling and current cooling at (a) 80 and (b) 10 K, respectively. The magnetic field is applied along the in-plane easy axis. The nearly identical initial magnetization curves indicate that current does not increase the volume fraction of the FMM phase.

the measurement. Apparently, the current-induced drop of resistivity is irreversible after a full cycle of current sweeping. This is especially true at 10 K, as the resistivity after the current cycle remains three orders of magnitude lower than that before the current cycle, indicating an irreversible change of the transport state in the film. In contrast, resistivity measured simultaneously in the perpendicular direction (dashed lines) drops by less than one order of magnitude in the same current cycle. At higher temperatures of 150 K, the change of the resistivity becomes more reversible and almost recovers the original value after the current cycle. The current-induced ($I = 2 \times 10^4$ A/cm$^2$) resistivity change can be quantified by CER $= [R(0) - R(I)]/R(I)$, which is calculated to be $2\,26\,800\%$, $26\,100\%$, and $43\%$ at 10, 80, and 150 K, respectively.

In stark contrast to its colossal effect on transport, the current appears to have little influence on the magnetic properties of the LPCMO films. Figures 2(a) and 2(b) show current ($2 \times 10^4$ A/cm$^2$) and zero-current cooling initial magnetization curves and *M-H* hysteresis loops at 80 and 10 K, respectively. Both the initial magnetization curve and the *M-H* loop look identical with and without current cooling. For the LPCMO system, it has been well known that the low field fast rise of the initial magnetization reflects the FMM part of the electronic phase separated the film. The fact that the current causes no change of the initial magnetization curve clearly indicates that the total volume fraction of the FMM phase is not affected by the current, despite the fact that the same current density induces more than three orders of magnitude drop of resistivity and 80 K increase of $T_{MIT}$.

Based on the fact that current causes a large change of conductivity without noticeably increasing the volume fraction of the FMM phase, one has to assume that the following two scenarios occur in the system: (1) the current reshapes
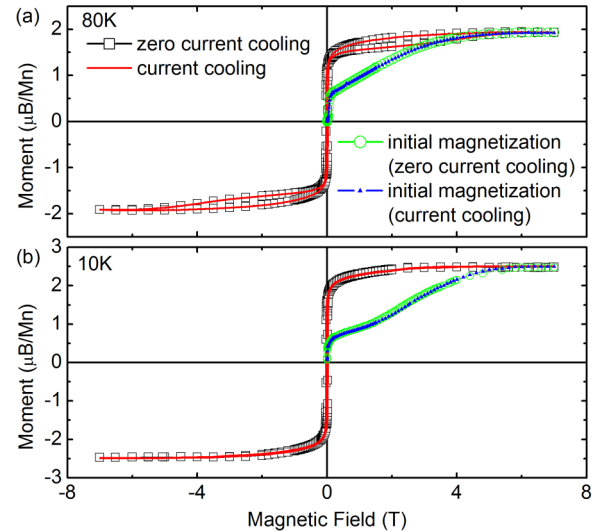
the FMM domains to become elongated along the current direction, which makes the percolation of FMM domains easier; (2) the current does not change the shape of the domains, but instead causes some tiny FMM domains to appear at certain critical regions along the conductive pathways. Both scenarios can result in large change conductivity but little change of total magnetization.

Our MFM studies unambiguously show that the latter scenario occurs in the LPCMO system. Figure 3 shows MFM images of the LPCMO film acquired from the same surface region [morphology shown in Fig. 3(a)] at 10 K (MFM image at 80 K shown in supplementary material [19]). A perpendicular field of 1000 Oe was applied during MFM imaging, which would yield some perpendicular components from the FMM domains for MFM imaging, but not strong enough to drive the COI state into the FMM state. In the MFM images, dark area (negative phase) and bright area (positive phase) represent FMM and COI phases, respectively [20]. Figure 3(b) shows MFM image acquired at 10 K after a zero-current cooling process. A series of MFM images are obtained after current cycles with different maximum current density [similar to Fig. 1(b)], as shown in Figs. 3(c) to 3(e). The FMM domains remain largely unchanged after the current cycles despite three orders of magnitude change of the resistivity. However, carefully comparing Figs. 3(b) to 3(e), one can see that after the current cycles a few small FMM domains appear to bridge otherwise unconnected FMM domains (e.g., marked by blue ellipse). The evolution of the tiny FMM domains with increasing maximum current density can be clearly seen in the magnified images in Fig. 3(f) (for more details see supplementary material [19]). For all current densities, the fraction of the newly appeared FMM "bridges" are negligible (less than 0.2% based on statistics) compared to the existing FMM domains, explaining why little change can be observed in global magnetization measurements. Similar phenomena
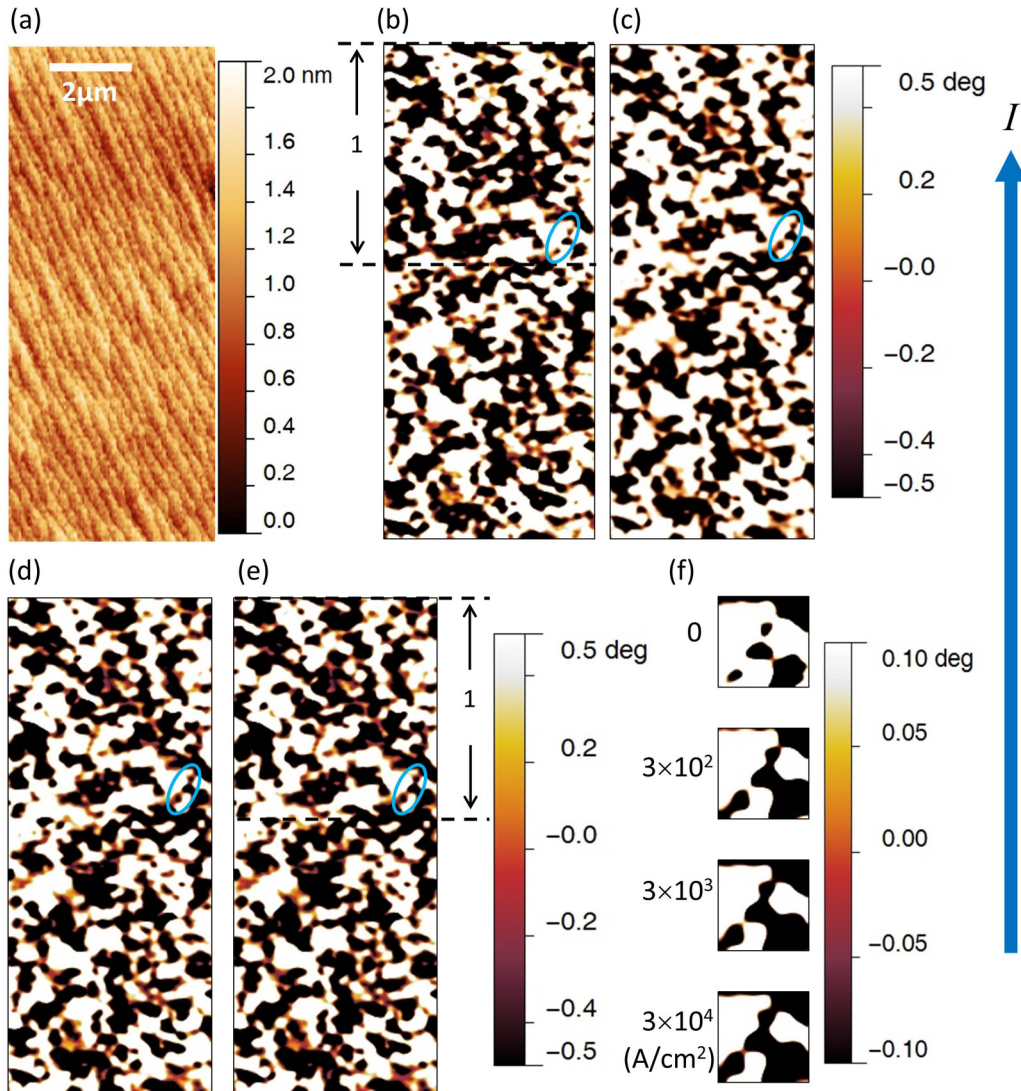
FIG. 3. The MFM images clearly show the shape of the FMM domains remain unchanged after current sweeping, while appearing a tiny fraction of FMM "bridges" as marked by the blue ellipses. (a) The AFM topography of the surface region where all MFM images were acquired. (b)-(e) are MFM images at virgin state and after different current sweeping at 10 K [the maximum current density for (c), (d), and (e) are $3 \times 10^2$, $3 \times 10^3$ and $3 \times 10^4$ A/cm$^2$, respectively]. (f) Magnified images of the corresponding ellipses marked regions.

are observed at 80 K, as shown in Fig. S4 [19], except the current-induced FMM "bridges" are more difficult to be observed by MFM, which is likely caused by the fact that the magnetization at 80 K is weaker than that at 10 K.

The observation of the current induced FMM "bridges" by MFM also explains the anisotropic behavior of the CER in Fig. 1(b). Because the formation of the tiny FMM domains have a preferential direction along the current direction, the drop of resistivity is expected to be much larger along current direction than that in the perpendicular direction. Indeed, as shown in Fig. 1(b), the measured horizontal resistivity (perpendicular to the sweeping current direction) drops by less than one order of magnitude, which is much smaller than the three orders of magnitude change along the current direction.

Finally, we use a resistor-network (RN) model [16,21–23] exactly based on the MFM results to show that the appearance of the few FMM "bridges" can result in more than three

orders of magnitude change of resistivity. In the RN model, $R_M$, $R_I$, $R_{MI}$ are used to denote the resistance of the joints between FMM-FMM, COI-COI, and FMM-COI, respectively. For simplicity, $R_{MI}$ is set as $(R_M + R_I)/2$. Based on previous measurements [15], the conductivity ratio between the FMM and the COI phase is estimated to be 100 000:1 at 10 K. The physical mechanism involved here does not quantitatively depend on the concrete values of $R_I$ and $R_M$ as long as $R_I \gg R_M$. The resistivity in the RN can then be exactly solved by the Kirchhoff equations. We chose one region in MFM image, marked as No. 1 in Figs. 3(b) and 3(e) (for more regions see supplementary material [19]). Figures 4(a) and 4(b) represent the No. 1 region before and after a large current cycle, in which a crucial conductive path is formed after current excitation (marked by blue ellipses). While the area fraction of the FMM phase is nearly the same in Figs. 4(a) and 4(b) (49.4% and 50.1%, respectively), the resistance is calculated to be 29 798 and 16.5 (arb unit) for Figs. 4(a) and 4(b), respectively.
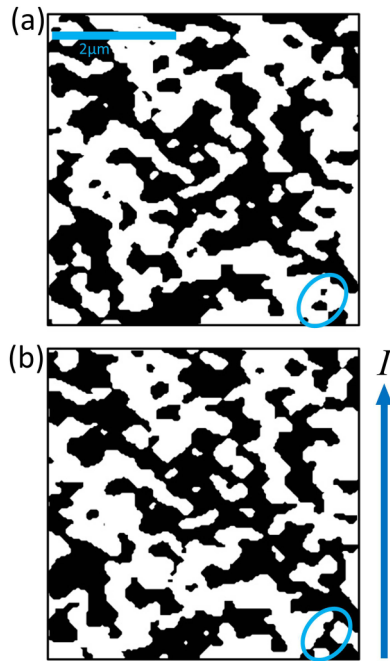
FIG. 4. The resistive network model simulations based on MFM images. Black area and white area represent FMM and COI phase, respectively. Panels (a) and (b) are conductive domain maps of No. 1 region before and after a current cycle at 10 K. The blue ellipses mark the conductive path induced by the current.

This is more than three orders of magnitude in difference, which is consistent with our transport data. We note that CER only occurs when the area fraction of the FMM phase is near percolation regime ($\sim$50%), and at higher temperatures the area fraction of FMM phase becomes significantly smaller and ER becomes small accordingly [Fig. 1(d)].

In summary, our work uncovers the underlying mechanism of the colossal electroresistance in the LPCMO system. In contrast to the previous belief that current reshapes the FMM domains, we show that the FMM domains remain virtually unchanged after passing electric current. Instead, it is the appearance of a tiny fraction of FMM "bridges" that changes the total conductivity dramatically. This also solves the puzzle why current induces a dramatic change of resistivity but little change of magnetization in the LPCMO system.

[1] T. Z. Ward, S. Liang, K. Fuchigami, L. F. Yin, E. Dagotto, E. W. Plummer, and J. Shen, Phys. Rev. Lett. **100**, 247204 (2008).

[2] W. D. Wu, C. Israel, N. Hur, S. Y. Park, S. W. Cheong, and A. Lozanne, Nat. Mater. **5**, 881 (2006).

[3] H. W. Guo, J. H. Noh, S. Dong, P. D. Rack, Z. Gai, X. S. Xu, E. Dagotto, J. Shen, and T. Z. Ward, Nano Lett. **13**, 3749 (2013).

[4] S. Duhalde, M. Villafuerte, G. Juárez, and S. P. Heluani, Phys. B **354**, 11 (2004).

[5] F. X. Hu and J. Gao, J. Appl. Phys. **99**, 08Q314 (2006).

[6] H. Y. Hwang, S. W. Cheong, P. G. Radaelli, M. Marezio, and B. Batlogg, Phys. Rev. Lett. **75**, 914 (1995).

[7] T. Z. Ward, J. D. Budai, Z. Gai, J. Z. Tischler, L. F. Yin, and J. Shen, Nat. Phys. **5**, 885 (2009).

[8] A. Sacchetti, T. Corridoni, E. Arcangeletti, and P. Postorino, Eur. Phys. J. B **66**, 301 (2008).

[9] Z. G. Sheng, Y. P. Sun, J. M. Dai, X. B. Zhu, and W. H. Song, Appl. Phys. Lett. **89**, 082503 (2006).

[10] J. M. Dai, W. H. Song, J. J. Du, J. N. Wang, and Y. P. Sun, Phys. Rev. B, **67**, 144405 (2003).

[11] M. Tokunaga, Y. Tokunaga, and T. Tamegai, Phys. Rev. Lett. **93**, 037203 (2004).

[12] A. Asamitsu, Y. Tomioka, H. Kuwahara, and Y. Tokura, Nature (London) **388**, 50 (1997).

[13] J. R. Sun, G. J. Liu, S. Y. Zhang, H. W. Zhang, X. F. Han, and B. G. Shen, Appl. Phys. Lett. **86**, 242507 (2005).

[14] J. Stankiewicz, J. Sesé, J. García, J. Blasco, and C. Rillo, Phys. Rev. B **61**, 11236 (2000).

[15] G. Garbarino, M. Monteverde, C. Acha, P. Levy, M. Quintero, T. Y. Koo, and S. W. Cheong, Phys. B **354**, 16 (2004).

[16] S. Dong, H. Zhu, and J. M. Liu, Phys. Rev. B **76**, 132409 (2007).

[17] Y. B. Liu, J. R. Sun, and B. G. Shen, J. Appl. Phys. **114**, 193704 (2013).

[18] H. Jeen and A. Biswas, Phys. Rev. B **88**, 024415 (2013).

[19] See Supplemental Material at http://link.aps.org/supplemental/10.1103/PhysRevB.93.035111 for sample preparation, structure, MFM, and simulation information.

[20] K. Du, K. Zhang, S. Dong, W. G. Wei, J. Shao, J. B. Niu, J. J. Chen, Y. Y. Zhu, H. X. Lin, X. L. Yin, S. H. Liou, L. F. Yin, and J. Shen, Nat. Commun. **6**, 6179 (2015).

[21] M. Mayr, A. Moreo, J. A. Vergés, J. Arispe, A. Feiguin, and E. Dagotto, Phys. Rev. Lett. **86**, 135 (2001).

[22] S. Dong, H. Zhu, X. Wu, and J. M. Liu, Appl. Phys. Lett. **86**, 022501 (2005).

[23] S. Ju, T. Y. Cai, and Z. Y. Li, Phys. Rev. B **72**, 184413 (2005).